Chromatographia (2016) 79:1197–1205
DOI 10.1007/s10337-016-3126-9

ORIGINAL

Compound-Specific Isotope Analysis of Amino Acid Labeling with Stable Isotope Nitrogen (^{15}N) in Higher Plants

Zhongyi Zhang[1,2] · Huayun Xiao[1] · Nengjian Zheng[1,2] · Xiaofei Gao[1,3] · RenGuo Zhu[1]

Received: 13 April 2016 / Revised: 12 June 2016 / Accepted: 17 June 2016 / Published online: 8 July 2016

Abstract Individual free amino acid δ^{15}N values in plant tissue reflect the metabolic pathways involved in their biosynthesis and catabolism and could thus aid understanding of environmental stress and anthropogenic effects on plant metabolism. In this study, compound-specific nitrogen isotope analysis of amino acid by gas chromatography-combustion-isotope ratio mass spectrometry (GC-C-IRMS) was carried out to determine individual free amino acid δ^{15}N values. High correlations were observed between the δ^{15}N values obtained by GC-C-IRMS and elemental analyzer-isotope ratio mass spectrometry (EA-IRMS) determinations, and the mean precision measured was better than 1 ‰. Cation-exchange chromatography was employed to purify the sample, and the difference between prior to and following passage through the resin was within 1 ‰. The amino acid δ^{15}N values of plant leave samples following incubation in ^{15}N-nitrate at different time points were determined. A typical foliar free amino acid ^{15}N-enrichment pattern was found, and glutamine was the most rapidly labeled amino acid; other amino acids derived from the GS-GOGAT cycle were also enriched. The pyruvate family amino acids were labeled less quickly followed by the aromatic amino acids. This study highlighted that amino acid metabolism pathways had a major effect on the δ^{15}N values. With the known amino acid metabolism pathways and δ^{15}N values determined by the presented method, the influence of various external factors on the metabolic cycling of amino acid can be understood well.

Keywords GC-C-IRMS · Free amino acid · ^{15}N-labeling · δ^{15}N

✉ Huayun Xiao
huayunxiao@outlook.com

[1] State Key Laboratory of Environmental Geochemistry, Institute of Geochemistry, Chinese Academy of Sciences, Guiyang 550081, China

[2] University of Chinese Academy of Sciences, Beijing 100039, China

[3] Aquatic Ecohealth Group, Key Laboratory of Urban Environment and Health, Institute of Urban Environment, Chinese Academy of Sciences, Xiamen 361021, China

Introduction

Plants are sessile, unable to relocate when exposed to diverse environmental (i.e., drought, salinity, cold, pollutants, and oxidative stress) and seasonal stimulation [1, 2], hence they have to respond rapidly to survive stress conditions by adapting their physiological and metabolic processes, in particular, the carbohydrate and amino acid metabolism [3–6]. Amino acid metabolism plays an important regulatory role in plant growth and adaptive responses to various environmental stresses, not only because amino acids are potential regulatory and signaling molecules, but also the precursors for energy-associated and numerous secondary metabolites [3, 7–9]. Amino acid can be grouped into families on the basis of metabolic intermediates that serve as their precursors. It is important to note that the specific amino acid family pathway responds differentially following different growth phase and stress conditions, and different pathways of amino acid families respond differentially even under similar stress conditions according to their physiological functions [5, 10–12]. Although several models describing amino acid metabolic pathway changed under environmental stress have previously been described on the basis of amino acid levels, it could not provide enough information about the actual activity of amino acid family pathway involved [5, 10, 13, 14]. Individual amino

acid $\delta^{15}N$ values in plant tissues can reflect the cycling of N into and within amino acids and could thus aid understanding of environmental and anthropogenic effects on plant amino acid metabolism [6, 15–18].

Compound-specific nitrogen isotope analysis (CSIA) of amino acid has been widely applied in biochemistry, archaeology, geochemistry, and ecology to determine the biosynthesis and catabolism pathway of amino acids. Besides, it is a powerful tool for estimating the trophic level of organisms and nitrogen flow in food webs. The application of stable nitrogen isotope ratio analysis for authenticity testing of organic products has also been largely investigated [19–25]. Compared with liquid chromatography-isotope ratio mass spectrometry (LC/IRMS), GC/C/IRMS is now considered to be the most suitable technique for measuring individual amino acid $\delta^{15}N$ values, owning to its high precision, sensitivity, and accuracy [26, 27], and it allows the determination of the isotope composition of C and N of amino acids in the range of natural abundance or slightly enriched samples. The major limitation of LC/IRMS is that the two commercial interfaces, LC-Isolink and LiquiFace, do not allow the measurement of $\delta^{15}N$ values [28, 29]. Recently, a novel high-temperature combustion interface for CSIA of both carbon and nitrogen via LC/IRMS is developed, and the highly efficient system will probably open up new possibility in CSIA-based research fields [30]. Therefore, the CSIA of free amino acid nitrogen isotope is carried on an available GC/C/IRMS system in this study.

However, the polar nature of amino acid requires derivatization prior to GC separation via replacement active hydrogen on carboxyl, amino, and certain side-chain polar functional groups with a nonpolar moiety. The goal of derivatization is to make amino acid more volatile, less reactive, and thus improve its chromatographic behavior [31, 32]. In the case of amino acid, silylation is a very powerful and convenient single-step derivatization strategy which can be carried out without additional cleaning of the reaction products [33–35]. Moreover, the alkaline milieu of this reaction allows the simultaneous measuring of glutamate and aspartate as well as their amides, glutamine, and asparagine [35, 36]. The main disadvantage of this method is its sensitivity to moisture. The presence of moisture results in poor reaction yield and instability of the derivatized analytes, in addition, change the $\delta^{15}N$ values of the individual amino acid. Therefore, any samples before silylation derivatization must be dried sufficiently [35].

As an aim to clarify ^{15}N distribution among free amino acid, we take the advantage of gas chromatography/combustion/isotope ratio mass spectrometry technique to measure the free amino acid $\delta^{15}N$ values under well-defined environmental conditions. The plant was incubated with [^{15}N-Potassium nitrate, 10.6 % atom ^{15}N], and the fraction of amino acid was purified by cation-exchange chromatography. Data showed that the highest $\delta^{15}N$ values were found for glutamine at each harvest time point, followed by amino acids derived from GS/GOGAT cycle.

Experimental

Chemicals and Materials

All amino acids, such as cation-exchange resin (Dowex 50 W × 8 H^+, 200–400 mesh size), pyridine (Py), and *N*-methyl-*N*-(*tert*-butyldimethylsilyl) trifluoroacetamide (MTBSTFA), used in the study were obtained from Sigma-Aldrich (St. Louis, MO, USA) in the highest purity grade available. All other solvents and reagents used were of HPLC grade and purchased from Aladdin (Shanghai, China). Ultrapure water was obtained in the laboratory using a Milli-Q water purification system (Millipore, Billerica, MA, USA) for the preparation of all solutions.

Plants and Growth Conditions

Orychophragmus violaceus was grown from seeds in raising seedling dish containing a 70:30 mixture (v/v) of horticultural substrate and perlite in a greenhouse under natural light and temperature. Twenty days after germination, young seedlings were transferred to plastic pots (15 cm in diameter and 15 cm tall) filled with 2700 g clay calcareous soil collected from the karst hills in Guizhou Province, China. Plants were grown outside under a rain shelter and watered well.

Introduction of Labeling and Sampling

Isotope labeling experiment was carried out a month later after transfer. The introduction of ^{15}N-labeling was performed on six pots of plants with the similar growth condition by adding 20 mL [^{15}N-Potassium nitrate, 10.6 % atom ^{15}N] at a final concentration of 5 g L^{-1}. Potassium nitrate was selected, because it generally served as nitrogen source and taken up by the roots. Leave samples were then harvested at different time points (0, 1, 3, 6, 12, and 24 h) after the addition of ^{15}N-Potassium nitrate. A control experiment with the addition of potassium nitrate at the $\delta^{15}N$ values of 20.1 ± 0.6 ‰ was also carried out. Because the free amino acid concentrations varied from leaf to leaf and changed with the age of plant, precaution was taken to harvest leaves of similar age, size, and position. Leave samples were washed three times with pure water and frozen immediately in liquid nitrogen, and then, they were grounded to a fine powder in liquid nitrogen.

Free Amino Acids Extraction, Derivatization, and Isotopic Analysis

The extraction and analysis of amino acid were carried out after Molero et al. (2011). Briefly, about 100 mg of leaf powder was homogenized with 1 mL of trifluoroacetic acid (TFA) 10 % (v/v) under sonication for 10 min at 4 °C. The homogenate was centrifuged at 14,000 *g* for 10 min at 4 °C. To recover the maximum amount of amino acid from the powder samples, the extraction procedure was repeated twice. The supernatant was collected and purified with Ultrafree-MC 1000 NMWL tubes (Millipore, USA). The purified supernatant was used for amino acids δ^{15}N values analysis, and 100 μL of α-amino butyric acid solution (2 mmol L^{-1}) was added as an internal reference ($\delta^{15}N = 8.43 \pm 0.03$ ‰). The supernatant was dried with an N_2 flow and kept at −80 °C before the analysis. The samples were resuspended in 2 mL of HCl 0.1 M (v/v), and the amino acid fraction was isolated using cation-exchange resin (Dowex 50 W X8 H^+, 200–400 mesh size; Sigma-Aldrich) filled in a chromatographic column. The amino acid-enriched fraction was obtained by elution with three bed volumes of 10 wt% NH_3 aqueous solution and dried sufficiently in preparation for the subsequent derivatization. The possible background compounds derived from the cation-exchange resin were also examined by blank procedures. Samples were then derivatized with 50 μL pyridine and 50 μL of *N*-methyl-*N*-(tert-butyldimethylsilyl) trifluoroacetamide (MTBSTFA), and incubated at 80 °C for 1 h. Under the reaction conditions used, most of the amino acids produced only one derivative with the exception of tryptophan, as shown in Fig. 1.

Individual amino acid nitrogen isotopic analysis was carried out using a Trace GC Ultra (GC IsoLink + ConFlo IV, Thermo Scientific, Bremen, Germany) interfaced with a Thermo Scientific MAT253 (Bremen, Germany). Chromatography was carried out with a DB-5 ms column (30 m × 0.25 mm × 0.25 μm; J&W Scientific, Folsom, CA, USA). Helium was used as the carrier gas for separation at a flow rate of 1.2 mL min^{-1}. For the δ^{15}N analysis, 1.0 − 1.5 μL of each sample was injected in splitless mode by an autosampler (Triplus, Thermo Scientific, Bremen, Germany) at an injector temperature of 270 °C. The temperature program used was 90 °C for 1 min, ramping at 8 °C min^{-1} to 140 °C for 5 min, then ramping at 3 °C min^{-1} to 220 °C and finally ramping at 12 °C min^{-1} to 285 °C, holding for 12.5 min. To prevent solvent from entering the combustion interface (and ion source), the system was "back flushed" with helium for about 900 s at the beginning, thus protecting the lifetime of the catalyst reactor. Once separated from a compound mixture, individual amino acid was converted online into CO_2, N_2, and H_2O in a new commercial NiO tube/CuO–NiO combustion reactor

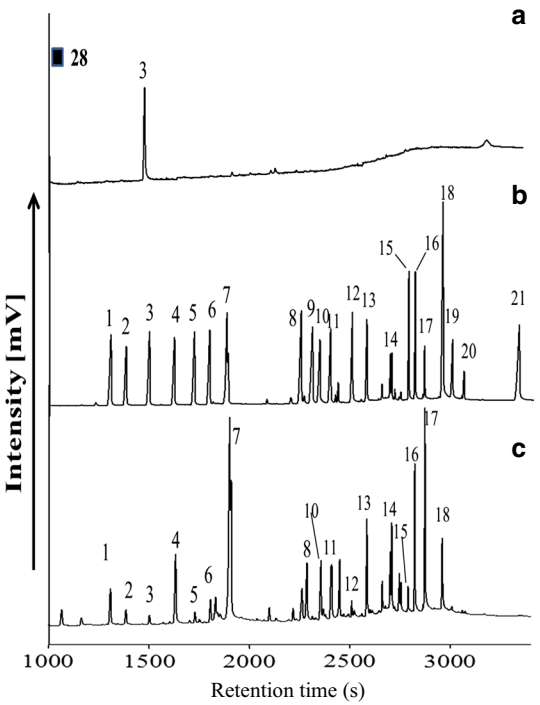

Fig. 1 GC-C-IRMS chromatogram for the analysis of tBDMSi derivatives. **a** Internal standard after passing through cation-exchange resin. **b** Amino acid standard mixture. **c** Leaves sample of *Orychophragmus violaceus. Peaks 1* Ala; *2* Gly; *3* I.S. (Aaba); *4* Val; *5* Leu; *6* Ile; *7* Pro; *8* Asn; *9* Met; *10* Ser; *11* Thr; *12* Phe; *13* Asp; *14* Glu; *15* Lys; *16* Gln; *17* Arg; *18* His; *19* Tyr; *20* Trp (2TMS); *21* Trp (3TMS)

which contained an Ni tube with an oxidized surface that displays a greater surface area compared with the conventional model, and it was operated at 1030 °C. Since this reactor contained an oxidation and a reduction unit (the Ni/NiO surface withdraws oxygen from nitrogen oxides thereby acting like a reduction catalyst), no extra reduction reactor was necessary for nitrogen measurements. Water vapor was removed by a water-removing trap, consisting of a Nafion membrane. During the δ^{15}N analysis, a liquid nitrogen trap was added after the combustion oxidation reactor to remove CO_2 from the oxidized and reduced analytes.

A standard mixture of all amino acids, whose δ^{15}N values were individually determined by EA-IRMS (Thermo Fisher Scientific, Bremen, Germany), was derivatized and the δ^{15}N values were measured by GC-C-IRMS at the beginning and at the end of daily measurement series as a quality control for consistent measurement conditions. Moreover, the isotopic value of the internal standard α-amino butyric acid added to each sample was checked. α-Amino butyric acid was chosen as internal standard, because it was not naturally present and separated well with other amino acids. The analytical run was accepted

when the differences of α-amino butyric acid between GC-C-IRMS and EA-IRMS values were at most ±1.5 ‰ for natural abundance or in slightly ^{15}N-enriched samples.

All δ^{15}N values were reported relative to a laboratory reference tank of high-purity molecular nitrogen (99.998 %). This was introduced directly into the ion source in four pulses at the beginning and end of each run. All samples were measured in duplicate, and the isotope ratios were expressed in δ ‰ versus atmospheric nitrogen.

Data acquisition on the IRMS instrument was carried out using Isodata 3.0 (Thermo Fisher Scientific, Bremen, Germany). Slope sensitivity for peak start and stop definition was set to be 0.2 and 0.4 mV s^{-1}, respectively. Integration time was 0.25 s.

Results and Discussion

Derivatization Procedure and Precondition GC-C-IRMS for δ^{15}N Analysis

Amino acids are not suitable for separation by gas chromatography until their carboxyl, amino, and certain side-chain functional groups have been chemically modified, among all the five derivatization reactions to our knowledge [16, 19, 33, 37–40], silylation via MTBSTFA is simple, single-step, highly reproducible and effective. More particularly, the alkaline milieu of the reaction allows the simultaneous recording of glutamate and aspartate as well as their corresponding amides, and histidine could only be measured using this derivatization procedure [33, 41]. The accurately determination of δ^{15}N in glutamine is very important for the comprehension of nitrogen cycling into and within the plants, since it is the branch point for nitrogen metabolism [6]. However, the main disadvantage of this method is the sensitivity of MTBSTFA to moisture, and the presence of moisture results in poor reaction yield and instability of the derivatived amino acids. To prevent the moisture, approximately 200 μg of anhydrous sodium sulfate (Na_2SO_4) was added to the dried samples before the derivatization procedure. As mentioned above, the majority of the amino acid produced only one derivative with the exception of tryptophan under our reaction conditions at 80 °C for 1 h (Fig. 1); the active hydrogens on hydroxyl, amine of amino acid were replaced by *N*(*O*)-(*tert*-butyldimethylsilyl) (TBDMS). It has been reported that appropriated modification of the reaction condition such as increasing the reaction time would resulted in an increased response of the fully derivatized form of tryptophan [35]. It should be noted that further effort was not made in this study, since the two derivative of tryptophan could be baseline separated completely.

The amino acids were successfully converted into TBDMS derivatives and could be completely resolved within 57 min by GC-C-IRMS. However, the presence of SiO_2 owing to the combustion of TBDMS derivatives in GC/C/IRMS would decrease the efficiency of the reactor, leading to a loss of sensitivity [34, 35, 38, 41]. The retention times of amino acids drifted, the signal intensity significantly decreased, and the δ^{15}N value tended to be enriched during the analysis. To solve these problems, only 8–9 runs were carried out in each sequence then a re-oxidation event of the reactor over a period of 10 min, and back-flush for 1 h was undertaken at the end of each sequence [42]. The retention times and signal intensities were retrieved on the following sequence, yet a reactor/instrument system conditioning phase with a run of amino acid mixtures was necessarily to offsets the ^{15}N-depletion drift caused by oxidation events [42, 43]. Once the GC-C-IRMS is perfectly set up (i.e., focus, tested for N_2 leaks, ref gas stability, etc.), the samples are measured as described above. The standard mixtures of amino acids may be measured only at the beginning and at the end of daily measurement series as a quality control for consistent measurement conditions.

Accuracy and Precision of GC-C-IRMS

To test the accuracy of the determination of amino acid isotopic values, we compared the δ^{15}N values of amino acids standards measured by GC-C-IRMS with the isotopic values of high-purity nonderivatized single amino acid obtained by EA-IRMS. The δ^{15}N values determined by EA-IRMS were the mean of three measurements, whereas the δ^{15}N values determined by GC-C-IRMS were the average of six runs. Figure 2 showed that the δ^{15}N values determined by EA-IRMS were linearly correlated with those determined by GC-C-IRMS after derivatization (R^2 = 0.982,

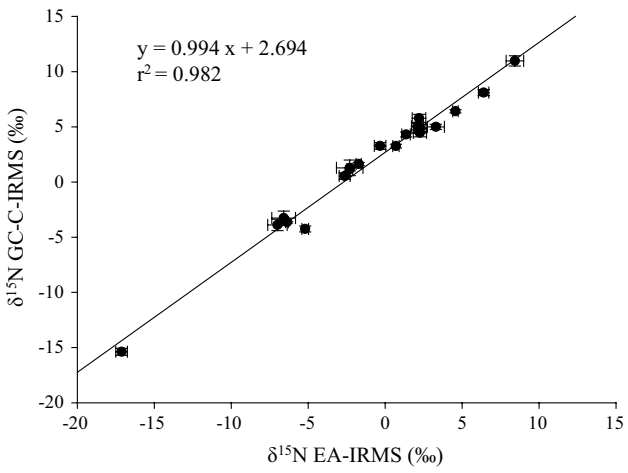

Fig. 2 Correlation between δ^{15}N values of amino acid standards determined by EA-IRMS and GC-C-IRMS. *Error bars* represent the SD of repeated measurements

Table 1 Percentage recovery and the isotopic composition of N (δ^{15}N ‰) of the standard amino acids

Amino acid	GC-C-IRMS							EA-IRMS	
	After Dowex resin				Before Dowex resin				
	Recovery	σ	δ^{15}N	σ	δ^{15}N	σ	Δ^a	δ^{15}N	Δ^b
Alanine	102.9	1.1	−6.76	0.8	−5.99	0.8	0.76	−6.63	0.58
Glycine	96.5	0.7	1.00	0.4	1.62	0.3	0.62	1.36	0.28
Valine	98.3	0.4	−0.14	0.5	0.58	0.4	0.72	−0.33	0.91
Leucine	95.5	1.4	1.62	0.5	2.36	0.4	0.74	2.10	0.26
Isoleucine	94.3	0.6	−2.03	0.2	−2.17	0.4	−0.14	−2.63	0.46
Proline	101.4	0.7	2.04	0.6	2.31	0.6	0.27	3.31	1.00
Methionine	98.7	1.8	−1.90	0.7	−1.06	0.2	0.84	−1.72	0.66
Serine	100.9	0.9	1.16	0.4	1.77	0.4	0.61	2.26	0.51
Threonine	93.4	0.6	0.58	0.5	0.56	0.2	−0.02	0.70	−0.14
Phenylalanine	92.1	0.2	1.47	0.6	2.20	0.5	0.73	2.28	−0.08
Aspartic acid	96.4	0.8	−1.89	0.3	−1.42	0.9	0.47	−2.32	0.90
Glutamic acid	96.4	2.5	−6.31	0.6	−6.98	0.2	−0.67	−5.15	−1.83
Asparagine	99.5	1.9	5.12	0.7	5.44	0.3	0.32	6.39	−0.95
Glutamine	95.2	0.5	−2.41	0.9	−1.54	0.2	0.86	−2.33	0.79
Lysine	93.1	3.1	2.23	0.3	3.10	0.4	0.87	2.23	0.87
Arginine	95.8	0.4	−5.78	0.7	−6.28	0.6	−0.50	−6.95	0.67
Histidine	94.7	0.7	−5.59	0.3	−6.37	0.1	−0.78	−6.38	0.01
Tyrosine	98.9	0.3	3.86	0.5	3.74	0.2	−0.12	4.57	−0.83
Tryptophan	90.4	0.5	−17.73	0.2	−18.19	0.5	−0.46	−17.13	−1.06

Δ^a Difference in δ^{15}N values of amino acids standard mixture directly analyzed and passed through an cation-exchange chromatography

Δ^b Difference in δ^{15}N values determined by EA/IRMS and GC/C/IRMS

$p < 0.001$), and the average absolute value of the offset between the values measured by EA-IRMS and by GC-C-IRMS after empirical correction was 0.7 ‰. The difference between the values measured by EA-IRMS and by GC-C-IRMS after empirical correction was not higher than ±1 ‰ (Table 1), with the exception of glutamate and tryptophan. Usually, two different peaks appeared for tryptophan in the GC-C-IRMS analysis under our reaction condition (Fig. 1), approving that they may underwent fractionation during the silylation reaction. The highest offset of glutamate between EA-IRMS and GC-C-IRMS may be due to the changed peak shape observed in GC-C-IRMS analyzes.

To evaluate the precision, three replicates of the reference amino acid mixtures were derivatized, and each of them was analyzed by GC-C-IRMS in triplicate. The precision (1σ) of GC-C-IRMS for any amino acid was less than 0.9 ‰ (Table 1).

Pretreatment of Amino Acids with Cation-Exchange Chromatography

Since accurate compound-specific isotope ratios analysis can be carried out only after true baseline resolution of adjacent compound peaks in the GC-C-IRMS chromatogram [1, 2], for the compounds of interest which were not well-resolved from each other or from the impurities present in the sample, an artificial enrichment of the preceding peak in δ^{15}N and the depletion of the following compound during the separate integration of peaks areas would occur. It is important, therefore, that sample extracts would be purified before the analysis [3, 4]. Pre-treatment of the sample extract with strong cation-exchange resins was known to be an efficient way to separation amino acids from complex hydrophilic compounds, such as sugars, organic acids, which consumed derivatization regents and also made damage to the combustion and reduction furnaces in the GC-C-IRMS system [5–8]. Molecular biology grade or biotechnology grade of Dowex 50 W X8 (200–400 mesh) resin was applied during our pre-treatment procedure; however, precise pre-wash treatment for resin was required to eliminate background contamination signals [44].

To examine possible background compounds derived from the cation-exchange resin, the pre-treatment procedure was applied to the analysis of the internal standard and monitored using GC-C-IRMS. No significant background compounds appeared in the chromatogram, even when a 10 % NH_3 aqueous solution was used in the final elution step (Fig. 1).

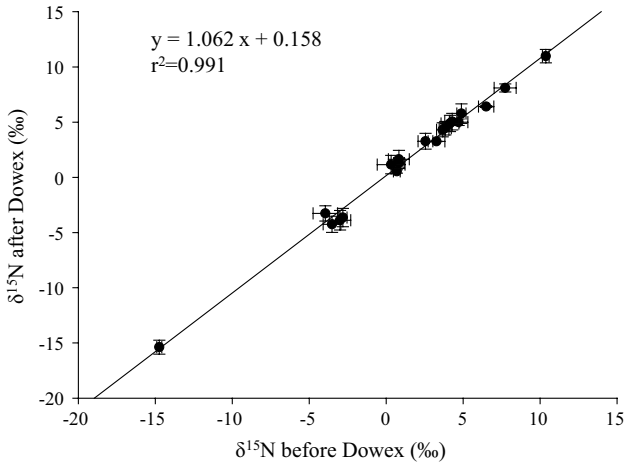

Fig. 3 Correlation between $\delta^{15}N$ values of amino acid standards determined by GC-C-IRMS before and after Dowex cation-exchange resin treatment. *Error bars* represent the SD of repeated measurements

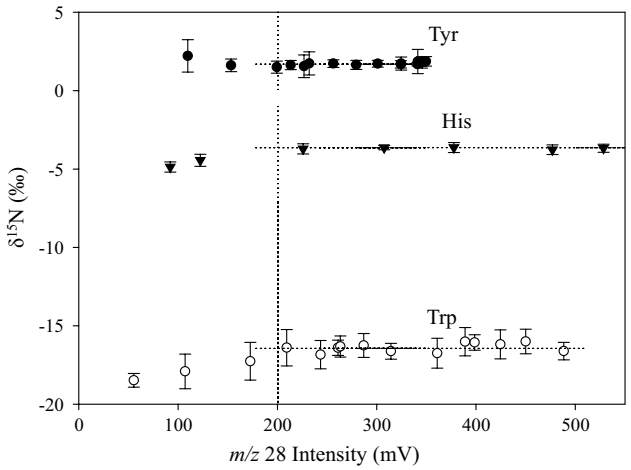

Fig. 4 Determined $\delta^{15}N$ values of Tyr, His, and Trp for various sample amounts. *Error bars* represent the SD of repeated measurements

The average recovery ratios of the amino acids before and after cation-exchange chromatography determined using gas chromatography with flame ionization detection (GC/FID) as their *N*(*O*)-(*tert*-butyldimethylsilyl) derivatives were shown in Table 1. The average recovery of amino acids using the present pre-treatment procedure was 96.5 %. We also compared nitrogen isotopic composition for the standard amino acids in mixtures before and after the cation-exchange pre-treatment procedure; there was no statistical difference between amino acid $\delta^{15}N$ values before and after the resin treatment. Figure 3 showed consistency of $\delta^{15}N$ values for the amino acid standards prior to and following passed through the cation-exchange resin. Although cation-exchange resin treatment may lead to a modification of $\delta^{15}N$ [26, 35, 43–45], in our study, the difference in $\delta^{15}N$ values before and after passing through the Dowex cation-exchange resin was lower than ±1 ‰.

Sample Requirements in Compound-Specific Isotope Analysis for $\delta^{15}N$

The amount required for the amino acids analysis in GC-C-IRMS is another important parameter that must be considered when optimizing the accuracy and precision of nitrogen isotope measurements. Chikaraishi et al. [46] reported that the limits of accurate measurement of the $\delta^{15}N$ values of amino acids can be carried out with the amplitudes ≥100 mV, corresponding to sample amounts larger than 30 ngN on column. Merritt and Hayes [37] also confirmed that the determined $\delta^{15}N$ values had a correlation with the sample amount.

The correlation between the determined $\delta^{15}N$ values and the sample amount was also confirmed in our study. Amount of 0.3–4.5 nmol amino acid standards were injected, and the correlations were shown in Fig. 4. Due to the difference in the IRMS instrument and the combustion reactor, the sample amount required in our study is not less than 15 ngN on column, and this roughly corresponding to an *m/z* 28 intensity of 200 mV.

Measurements of Amino Acid $\delta^{15}N$ Values in Leaves

To prevent the inter-run memory after a run of ^{15}N-enriched samples [47], a re-oxidation event of the reactor over a period of 10 min and back-flush for 1 h was undertaken. Interestingly, the internal standard which usually ranged between 10 and 12 ‰ of $\delta^{15}N$ also showed slightly enriched ^{15}N values due to an intra-run memory effect (Table 2). To our knowledge, method to minimize the intra-run memory effect has not yet been well verified, so we have not applied such method so far.

The results of Table 2 summarized the $\delta^{15}N$ abundance of amino acids extracted from the leaves during the 24 h time courses of labeling with [^{15}N-Potassium nitrate, 10.6 % atom ^{15}N]. Parts of the enriched $^{15}NO_3$ absorbed by root were delivered to the leaves and reduced by the leaf nitrogenase activity to the form of NH_4^+. The new fixed NH_4^+ was then incorporated into other amino acids. Therefore, a typical foliar free amino acids ^{15}N-enrichment pattern occurred as usually found after addition of ^{15}N–NO_3. The $\delta^{15}N$ values of the detectable amino acids increased with increasing ^{15}N–NO_3 labeling time.

In nitrogen metabolism of higher plants, glutamine is the first production in the conversion of inorganic form of nitrogen to organic form catalyzed by glutamine synthetase and the starting point for the synthesis of all other N-containing molecules that make up a cell [6, 48].

Table 2 δ^{15}N values of amino acids labeled in leaves following incubation in ^{15}N–NO_3 for 1, 3, 6, 12, and 24 h

Amino acid	1 h	3 h	6 h	12 h	24 h
δ^{15}N (‰)					
Glutamate	23.3 ± 1.6	148.1 ± 3.9	252.4 ± 2.8	614.1 ± 8.7	1807.1 ± 3.2
Glutamine	44.1 ± 0.1	236.3 ± 4.0	348.9 ± 3.4	500.3 ± 0.2	1287.5 ± 3.6
Arginine	3.7 ± 0.5	13.0 ± 0.8	14.0 ± 3.1	287.8 ± 0.5	786.3 ± 8.8
Proline	18.5 ± 0.1	107.7 ± 2.3	209.6 ± 7.8	586.2 ± 5.9	421.5 ± 4.8
Histidine	−1.3 ± 0.2	0.8 ± 1.6	56.3 ± 1.3	105.7 ± 7.2	123.9 ± 6.1
Aspartate	25.8 ± 1.8	207.5 ± 0.8	339.5 ± 1.5	743.9 ± 3.9	1971.0 ± 9.2
Asparagine	21.0 ± 2.0	92.9 ± 3.2	152.9 ± 1.8	361.1 ± 6.7	790.7 ± 4.1
Lysine	3.4 ± 1.3	9.2 ± 2.5	20.9 ± 2.2	64.4 ± 6.2	121.3 ± 4.3
Threonine	12.0 ± 0.1	26.5 ± 0.4	32.0 ± 3.7	127.3 ± 5.5	295.2 ± 6.3
Methionine	−1.7 ± 0.8	68.3 ± 2.9	181.3 ± 8.9	422.2 ± 4.6	281.4 ± 3.5
Isoleucine	1.9 ± 0.4	4.4 ± 2.6	45.5 ± 2.0	335.2 ± 3.2	303.2 ± 4.1
Alanine	21.8 ± 0.5	180.1 ± 4.9	279.6 ± 0.3	703.8 ± 7.9	1348.9 ± 5.1
Valine	9.1 ± 1.0	11.6 ± 2.1	35.8 ± 0.1	180.2 ± 7.5	195.1 ± 2.3
Leucine	15.6 ± 0.7	66.3 ± 1.8	121.5 ± 4.2	244.1 ± 1.9	194.4 ± 0.5
Tyrosine	11.6 ± 0.8	50.4 ± 0.7	140.8 ± 3.7	210.9 ± 2.4	326.1 ± 1.6
Tryptophan	−0.4 ± 0.1	5.1 ± 0.3	16.8 ± 1.8	64.5 ± 1.2	120.5 ± 2.2
Phenylalanine	10.0 ± 0.6	30.0 ± 1.4	76.8 ± 4.5	191.4 ± 9.2	261.4 ± 7.6
Serine	5.5 ± 0.9	125.1 ± 3.2	233.3 ± 4.5	542.3 ± 8.2	1279.8 ± 1.7
Glycine	−9.1 ± 0.2	21.3 ± 1.8	54.2 ± 4.1	81.5 ± 6.4	480.9 ± 9.5
I.S.	12.3 ± 0.9	13.8 ± 0.2	28.9 ± 1.7	32.0 ± 2.3	55.2 ± 3.1

Values are mean ± SD

Therefore, there was no doubt that the amino acids which derived from the GS-GOGAT cycle increased rapidly during the initial labeling period as observed from Table 2. The N-amide of glutamine was donated to the biosynthesis of many other important organic N compounds, so the net labeling level of glutamine was slowly at the later time. The high ^{15}N-enrichment patterns of amino acids which derived from the GS-GOGAT cycle (i.e., asparagine, glutamate, and aspartate) were also found following incubation with ^{15}N–NO_3. After 12 h of labeling period, glutamate became extensively labeled and greatly exceeded the isotopic abundance of glutamine. It can be rationalized that the GDH (glutamate dehydrogenase) pathway dominated in ammonia assimilation under N-saturated environment; GDH catalyzed the reductive amination of α-ketoglutarate to yield glutamate directly. The slow ^{15}N-enrichment of asparagine is, furthermore, in agreement with its function as N storage and transport substance.

Alanine was also labeled rapidly, suggesting that the assimilation pathway through transaminase occurred quickly in the leaves. Besides alanine, two other amino acids, leucine and valine, from the pyruvate family pathway showed less labeled rate during the labeling course, indicated that they would be utilized in the synthesis of proteins and other nitrogenous materials. Serine was more heavily labeled than glycine at all times during the labeling course, suggesting that glycine may be not the precursor of serine, although several study confirmed that they could interconvertible [49–51]. A pathway of serine synthesis from glycine would be expected to occur only during photorespiration. The aromatic amino acid family, which include tyrosine, phenylalanine, and tryptophan, were labeled less quickly; they may be synthesized from transamination of a less labeled primary assimilation product and converted quickly to secondly metabolism product. In this study, glutamate, glutamine, aspartate, alanine, and serine were the main labeled nitrogenous pools in leave tissue.

In the control experiment with the addition of potassium nitrate at the δ^{15}N values of 20.1 ‰, the δ^{15}N values of glutamate, glutamine, aspartate, alanine, and asparagine were also positive than the others, indicated that most of the inorganic nitrogen was assimilated by GS/GOGAT cycle in higher plants (Table 3).

These observations confirmed that the initial labeling patterns in the plant leaves were resulted from the utilization of nitrate transported from the root and then reduced and assimilated. The effect of amino acid metabolism pathways played a major factor in the δ^{15}N values of individual free amino acid; specific amino acid metabolism pathway was preferred or discriminated during assimilation of N–NO_3. Labeled nitrogen was incorporated into a range of free amino acids; the principal sinks for assimilation were alanine, aspartate, asparagine, glutamate, and glutamine.

Table 3 $\delta^{15}N$ values of amino acids in the control experiment following incubation in KNO_3 for 3, 12, and 24 h

Amino acid	3 h	12 h	24 h
Glutamate	6.0 ± 0.3	4.1 ± 0.7	3.6 ± 0.2
Glutamine	13.7 ± 0.2	11.6 ± 0.5	9.5 ± 0.1
Arginine	3.2 ± 1.1	1.8 ± 0.5	−0.3 ± 0.8
Proline	9.7 ± 1.4	4.2 ± 0.9	10.5 ± 0.7
Histidine	8.9 ± 0.8	9.7 ± 0.2	4.9 ± 0.3
Aspartate	11.8 ± 0.5	9.9 ± 0.4	9.0 ± 0.4
Asparagine	12.8 ± 0.3	11.1 ± 0.5	9.7 ± 0.8
Alanine	9.2 ± 1.8	5.2 ± 1.5	7.1 ± 0.7
Serine	2.7 ± 0.9	7.9.3 ± 1.5	13.0 ± 0.9
Glycine	−6.2 ± 0.9	−7.0 ± 1.1	−9.6 ± 0.6
I.S.	11.4 ± 0.6	11.8 ± 1.3	11.3 ± 0.9

Values are mean ± SD

Conclusion

In the present study, GC-C-IRMS was used to follow nitrogen assimilation and amino acid biosynthesis in the higher plant leaves. The derivatization method converted AAs to their TBDMS derivatives which enabled the measurement of $\delta^{15}N$ values of 18 free amino acids with high accuracy and precision, including glutamine and asparagine. Results also proved that the pretreatment with Dowex cation-exchange resin was a useful and reliable way to purify plant AAs. The treatment with Dowex cation-exchange resin had no significant effect upon the $\delta^{15}N$ values of amino acid mixtures; the difference prior to and following passage the resin was within 1 ‰. The amount of sample used in GC-C-IRMS was also optimized, and the sample amount required in our study is not less than 15 ngN on column.

The applicability of GC-C-IRMS for the determination of compound-specific nitrogen isotope of amino acid could be useful in our understanding of amino acid metabolism. We approved that the primary incorporation of $^{15}NO_3$ appears to proceed via the glutamine synthetase activity to glutamine. Meanwhile, alanine, aspartate, asparagine, glutamate, and serine were the main labeled nitrogenous pools; the aromatic amino acids were labeled less quickly followed by the pyruvate family in our study. With the known amino acid metabolism pathways and amino acid $\delta^{15}N$ values determined by the presented method, the influence of various external factors on the metabolic cycling of amino acid can be understood well.

Acknowledgments This study work was kindly supported by the National Natural Science Foundation of China through Grants 41425014, 41173027, 41273027 (H. Y. Xiao).

Compliance with ethical standards

Conflict of interest No conflict exists; all authors declare that they have no conflict of interest.

Ethical approval This article does not contain any studies with human participants or animal performed by any of the authors.

References

1. Mustroph A, Barding GA Jr, Kaiser KA, Larive CK, Bailey-Serres J (2014) Plant Cell Environ 37:2366–2380. doi:10.1111/pce.12282
2. Mahajan S, Tuteja N (2005) Arch Biochem Biophys 444:139–158. doi:10.1016/j.abb.2005.10.018
3. Miflin BJ, Lea P (1977) Ann Rev Plant Physiol 28:299–329
4. Suzuki N, Rivero RM, Shulaev V, Blumwald E, Mittler R (2014) New Phytol 203:32–43. doi:10.1111/nph.12797
5. Hildebrandt TM, Nunes Nesi A, Araujo WL, Braun HP (2015) Mol Plant 8:1563–1579. doi:10.1016/j.molp.2015.09.005
6. Styring AK, Fraser RA, Bogaard A, Evershed RP (2014) Phytochemistry 97:20–29. doi:10.1016/j.phytochem.2013.05.009
7. Binder S, Knill T, Schuster J (2007) Physiol Plant 129:68–78. doi:10.1111/j.1399-3054.2006.00800.x
8. Suzuki A, Knaff DB (2005) Photosynth Res 83:191–217. doi:10.1007/s11120-004-3478-0
9. Hausler RE, Ludewig F, Krueger S (2014) Plant Sci 229:225–237. doi:10.1016/j.plantsci.2014.09.011
10. Kirma M, Araujo WL, Fernie AR, Galili G (2012) J Exp Bot 63:4995–5001. doi:10.1093/jxb/ers119
11. Galili G (2011) Plant Signal Behav 6:192–195
12. Krasensky J, Jonak C (2012) J Exp Bot 63:1593–1608. doi:10.1093/jxb/err460
13. Harding HP, Zhang Y, Zeng H, Novoa I, Lu PD, Calfon M, Sadri N, Yun C, Popko B, Paules R, Stojdl DF, Bell JC, Hettmann T, Leiden JM, Ron D (2003) Mol Cell 11:619–633. doi:10.1016/s1097-2765(03)00105-9
14. Seifi HS, Van Bockhaven J, Angenon G, Hofte M (2013) Mol Plant Microbe Interact MPMI 26:475–485. doi:10.1094/MPMI-07-12-0176-CR
15. Gauthier PP, Lamothe M, Mahé A, Molero G, Nogués S, Hodges M, Tcherkez G (2013) Plant. Cell Environ 36:128–137
16. Molero G, Aranjuelo I, Teixidor P, Araus JL, Nogues S (2011) Rapid Commun Mass Spectrom RCM 25:599–607. doi:10.1002/rcm.4895
17. Xiao H-Y, Wu L-H, Zhu R-G, Wang Y-L, Liu C-Q (2011) Environ Pollut 159:363–367
18. Gallais A, Coque M, Quillere I, Prioul JL, Hirel B (2006) New Phytol 172:696–707. doi:10.1111/j.1469-8137.2006.01890.x
19. Styring AK, Sealy JC, Evershed RP (2010) Geochim Cosmochim Acta 74:241–251. doi:10.1016/j.gca.2009.09.022
20. Sabadel AJM, Woodward EMS, Van Hale R, Frew RD (2016) Food Webs 6:9–18. doi:10.1016/j.fooweb.2015.12.003
21. Styring AK, Fraser RA, Arbogast R-M, Halstead P, Isaakidou V, Pearson JA, Schäfer M, Triantaphyllou S, Valamoti SM, Wallace M, Bogaard A, Evershed RP (2015) J Archaeol Sci 53:504–515. doi:10.1016/j.jas.2014.11.009
22. Paolini M, Ziller L, Laursen KH, Husted S, Camin F (2015) J Agric Food Chem 63:5841–5850. doi:10.1021/acs.jafc.5b00662
23. Rubino M, Milin S, D'Onofrio A, Signoret P, Hatte C, Balesdent J (2014) Isot Environ Health Stud 50:516–530. doi:10.1080/10256016.2014.959444
24. Ohkouchi N, Tsuda R, Chikaraishi Y, Tanabe K (2012) Mar Biol 160:773–779. doi:10.1007/s00227-012-2132-1

25. Chikaraishi Y, Steffan SA, Ogawa NO, Ishikawa NF, Sasaki Y, Tsuchiya M, Ohkouchi N (2014) Ecol Evol 4:2423–2449. doi:10.1002/ece3.1103
26. Metges CC, Petzke KJ (1997) Anal Biochem 247:158–164
27. Matson P, Johnson L, Billow C, Miller J, Pu RL (1994) Ecol Appl 4:280–298. doi:10.2307/1941934
28. Moerdijk-Poortvliet TCW, Stal LJ, Boschker HTS (2014) J Sea Res 92:19–25. doi:10.1016/j.seares.2013.10.002
29. Krummen M, Hilkert AW, Juchelka D, Duhr A, Schluter HJ, Pesch R (2004) Rapid Commun Mass Spectrom RCM 18:2260–2266. doi:10.1002/rcm.1620
30. Federherr E, Willach S, Roos N, Lange L, Molt K, Schmidt TC (2016) Rapid Commun Mass Spectrom RCM 30:944–952. doi:10.1002/rcm.7524
31. Styring AK, Kuhl A, Knowles TD, Fraser RA, Bogaard A, Evershed RP (2012) Rapid Commun Mass Spectrom RCM 26:2328–2334. doi:10.1002/rcm.6322
32. Jimenez-Martin E, Ruiz J, Perez-Palacios T, Silva A, Antequera T (2012) J Agric Food Chem 60:2456–2463. doi:10.1021/jf2052338
33. Corr LT, Berstan R, Evershed RP (2007) Rapid Commun Mass Spectrom RCM 21:3759–3771. doi:10.1002/rcm.3252
34. Steven R, Shinebarger MH, Dwight E (2002) Matthews. Anal Chem 74:6244–6251
35. Hofmann D, Gehre M, Jung K (2003) Isot Environ Health Stud 39:233–244. doi:10.1080/1025601031000147630
36. Woo K-L, Chang D-K (1993) J Chromatogr A 638:97–107
37. Merritt DA, Hayes JM (1994) J Am SK Mass Spectrum 5:387–397
38. Walsh RG, He S, Yarnes CT (2014) Rapid Commun Mass Spectrom RCM 28:96–108. doi:10.1002/rcm.6761
39. Arkan T, Molnár-Perl I (2015) Microchem J 121:99–106. doi:10.1016/j.microc.2015.02.007
40. Montigon F, Boza J, Fay L (2001) Rapid Commun Mass Spectrom 15:116–123
41. Hofmann D, Jung K, Segschneider HJ, Gehre M, Schüürmann G (1995) Isot Environ Health Stud 31:367–375. doi:10.1080/10256019508036284
42. Reinnicke S, Juchelka D, Steinbeiss S, Meyer A, Hilkert A, Elsner M (2012) Rapid Commun Mass Spectrom RCM 26:1053–1060. doi:10.1002/rcm.6199
43. Molero G, Aranjuelo I, Teixidor P, Araus JL (2011) Rapid Commun Mass Spectrom 25:599–607
44. Takano Y, Kashiyama Y, Ogawa NO, Chikaraishi Y, Ohkouchi N (2010) Rapid Commun Mass Spectrom RCM 24:2317–2323. doi:10.1002/rcm.4651
45. Cayol M, Capitan P, Prugnaud J, Genest M, Beaufrere B, Obled C (1995) Anal Biochem 227:392–394
46. Chikaraishi Y, Takano Y, Ogawa NO, Ohkouchi N (2010) Earth Life Isot 300:365–386
47. Petzke KJ, Metges CC (2012) Rapid Commun Mass Spectrom RCM 26:195–204. doi:10.1002/rcm.5319
48. Newsholme P, Procopio J, Lima MM, Pithon-Curi TC, Curi R (2003) Cell Biochem Funct 21:1–9. doi:10.1002/cbf.1003
49. Ros R, Munoz-Bertomeu J, Krueger S (2014) Trends Plant Sci 19:564–569. doi:10.1016/j.tplants.2014.06.003
50. Munoz-Bertomeu J, Anoman A, Flores-Tornero M, Toujani W, Rosa-Tellez S, Fernie AR, Roje S, Segura J, Ros R (2013) Plant Signal Behav 8:e27104. doi:10.4161/psb.27104
51. Gauthier PP, Lamothe M, Mahe A, Molero G, Nogues S, Hodges M, Tcherkez G (2013) Plant Cell Environ 36:128–137. doi:10.1111/j.1365-3040.2012.02561.x